Mutation of the Highly Conserved Tryptophan in the Serpin Breach Region Alters the Inhibitory Mechanism of Plasminogen Activator Inhibitor-1†

Grant E. Blouse,*,‡,§ Michel J. Perron,‡ Jan-Olov Kvassman,|| Saadia Yunus,‡ Jannah H. Thompson,‡ Russell L. Betts,‡ Leonard C. Lutter,⊥ and Joseph D. Shore‡,§

Department of Pathology, Division of Biochemical Research, Henry Ford Health Sciences Center, Detroit, Michigan 48202, Department of Pharmacology, Wayne State University School of Medicine, Wayne State University, Detroit, Michigan 48201, Department of Chemistry and Biomedical Science, University of Kalmar, Kalmar, Sweden, and Molecular Biology Research, Henry Ford Health Sciences Center, Detroit, Michigan 48202

Received May 7, 2003; Revised Manuscript Received August 28, 2003

ABSTRACT: We have demonstrated that interactions within the conserved serpin breach region play a direct role in the critical step of the serpin reaction in which the acyl−enzyme intermediate must first be exposed to hydrolyzing water and aqueous deacylation. Substitution of the breach tryptophan in PAI-1 (Trp175), a residue found in virtually all known serpins, with phenylalanine altered the kinetics of the reaction mechanism and impeded the ability of PAI-1 to spontaneously become latent without compromising the inherent rate of cleaved loop insertion or partitioning between the final inhibited serpin−proteinase complex and hydrolyzed serpin. Kinetic dissection of the PAI-1 inhibitory mechanism using multiple target proteinases made possible the identification of a single rate-limiting intermediate step coupled to the molecular interactions within the breach region. This step involves the initial insertion of the proximal reactive center loop hinge residue(s) into β-sheet A and facilitates translocation of the distal P′-side of the cleaved reactive center loop from the substrate cleft of the proteinase. Substitution of the tryptophan residue raised the kinetic barrier restricting the initial loop insertion event, significantly retarding the rate-limiting step in tPA reactions in which strong exosite interactions must be overcome for the reaction to proceed.

Serpins are members of an expanding gene family, now identified in a spectrum of organisms ranging from viruses to multicellular eukaryotes (*1*, *2*) and, most recently, prokaryotes (*3*). The majority of serpins regulate key physiological pathways by inhibiting serine proteinases of the chymotrypsin-like fold (*1*, *4*−*6*); however, a few inhibit cysteine proteinases (*2*, *7*, *8*), and several are noninhibitory with likely roles as molecular chaperones (*1*, *2*). Despite a broad functional diversification and wide proteinase specificity, the extent of consensus sequence homology is remarkable, with each serpin sharing an evolutionarily conserved topology comprised of three β-sheets (A−C), typically nine α-helices and a flexible reactive center loop (RCL)[1] that confers target specificity (*1*, *2*, *9*). The mechanism of inhibition is quite novel and dependent upon a profound conformational change of the serpin topology, generally termed the "stressed" to "relaxed" (S → R) transition (*9*) in which target proteinases are kinetically trapped as stable acyl−enzyme complexes (*10*, *11*). Proteolysis of the P1−P1′ scissile bond initiates a concerted rearrangement of the serpin structure that involves an expansion of β-sheet A and rapid insertion of the cleaved RCL as an additional strand in β-sheet A (*12*). The conformational switch effectively transfers the covalently tethered proteinase from its initial docking site in the Michaelis complex to the opposite pole of the serpin, where distortion of the catalytic triad stabilizes the acyl−enzyme intermediate (*11*, *13*).

Recent progress concerning the nature of the serpin inhibition mechanism has been rather extensive, mostly focusing on the structural basis for the conformational change and the sequence of mechanistic steps describing the inhibitory pathway (*11*). However, relatively little is known with respect to conserved molecular interactions within the serpin

† This work was supported by National Institutes of Health Grant HL 54930 (to J.D.S.).

* To whom correspondence should be addressed: Division of Biochemical Research, Henry Ford Health Sciences Center, 1 Ford Place 5-D, Detroit, MI 48202-2689. Telephone: (313) 874-3228. Fax: (313) 876-2380. E-mail: gblouse1@hfhs.org.

‡ Division of Biochemical Research, Henry Ford Health Sciences Center.

§ Wayne State University.

|| University of Kalmar.

⊥ Molecular Biology Research, Henry Ford Health Sciences Center.

[1] Abbreviations: PAI-1, plasminogen activator inhibitor type 1; RCL, reactive center loop; tPA, tissue-type plasminogen activator; uPA, urokinase plasminogen activator; PAB, *p*-aminobenzamidine; PCR, polymerase chain reaction; SDS−PAGE, sodium dodecyl sulfate−polyacrylamide gel electrophoresis; P1−P1′ and P9, Schecter and Berger nomenclature for the reactive center loop residues of PAI-1, where P1, P2, P3, etc., and P1′, P2′, P3′, etc., denote those residues on the amino-terminal and carboxyl sides of the scissile bond, respectively; k_{app}, apparent second-order rate constant of proteinase inhibition; k_{assoc}, second-order association rate constant for Michaelis complex formation; k_{lim}, limiting rate constant; HEPES, 4-(2-hydroxyethyl)piperazine-1-ethanesulfonic acid; EDTA, ethylenediaminetetraacetic acid; NBD, *N*,*N*′-dimethyl-*N*-acetyl-*N*′-methyl(7-nitrobenz-2-oxa-1,3-diazol-4-yl)-ethylenediamine; Fmoc, 9-fluorenylmethyloxycarbonyl; DIPEA, *N*,*N*′-diisopropylethylamine; HBTU, *O*-benzotriazol-1-yl-*N*,*N*,*N*′,*N*′-tetramethyluronium hexafluorophosphate; TFA, trifluoroacetic acid; DMF, dimethylformamide.

10.1021/bi034737n CCC: $25.00
Published on Web 10/03/2003

FIGURE 1: Localization of the serpin breach region and the evolutionarily conserved tryptophan residue on the PAI-1 structure. The active (stressed) structure of PAI-1 is depicted with the position of the breach region indicated. The β-sheet structures are shown in yellow. α-Helices are shown in red. Reactive center loop residues P17−P5′ are shown in magenta. The conserved tryptophan residue (Trp175) is represented as a cpk-colored ball-and-stick model. This figure was generated in Swiss PDB Viewer (version 3.7) (*65*), using the coordinates for active PAI-1 (PDB entry 1B3K; chain A in ref *63*).

architecture that might play vital roles in regulating the mechanism of inhibition. Insight has come from several studies indicating that evolutionarily conserved amino acids cluster in well-defined areas related to the molecular mobility of the serpin molecule, suggestive of an involvement in the general mechanism of serpin action (*2*, *9*), whereas hypervariable residues appear to have contributed to the divergence of biochemical function and target specificity (*1*, *2*, *14*, *15*). Of particular interest to this study are those residues within the structural fold termed the breach region (*9*), comprising residues at the top of β-strands s3A and s5A and including those located on β-strands s2B−s4B (Figure 1). The location of the breach at the point for initial insertion of the cleaved reactive center loop and the fact that it bears the highest density of evolutionary conservation in the serpin fold reflect the critical importance of this structural motif (*2*, *9*). An evolutionarily conserved tryptophan found in virtually all reported serpin sequences (*2*, *3*) is positioned at the top of β-strand s3A in a hydrophobic pocket within the breach (Figure 1) and is tightly packed among several other highly conserved residues (*9*, *16*) shown to maintain critical hydrogen bonding networks in the structures of serpin 1K (*17*) and PAI-2 (*18*).

To better understand the molecular basis underlying an evolutionary conservation within the breach, we engineered a phenylalanine mutation at the position of the conserved tryptophan in PAI-1 (Trp175) (Figure 1). The functional significance of this conserved residue with regard to the individual kinetic steps in the reaction of PAI-1 with two physiologically relevant target proteinases, tPA and uPA, two nontarget proteinases, trypsin and elastase, and a mutant variant of tPA in which several basic residues in the exosite loop have been mutated to alanine, TNK-tPA (*19*−*21*), was assessed by fast reaction kinetics using stopped-flow and rapid acid quenching techniques. Evaluation of the individual kinetic constants determined for each step of the PAI-1 reaction made possible the identification of a rate-limiting step in the serpin inhibitory mechanism that was susceptible to alterations of the molecular environment within the breach region. For a serpin such as PAI-1, which has evolved extended exosite interactions with its primary target proteinases (*22*−*24*), release of the P′-side of the cleaved reactive center loop from the substrate pocket of the proteinase is thought to be rate-limiting (*25*, *26*). The findings presented here reveal that this particular transient step in the serpin reaction mechanism is critically dependent upon the structure of the serpin breach region.

EXPERIMENTAL PROCEDURES

Materials and Reagents. Unless otherwise indicated, all spectral and kinetic measurements were performed at pH 7.4 and 25 °C in a HEPES/NaCl reaction buffer with an ionic strength of 0.15 and containing 30 mM HEPES, 0.135 M NaCl, and 1 mM EDTA. Acrylic sample cuvettes were coated with 0.1% polyethylene glycol for reduction of the level of protein adsorption. The chromogenic substrates Spectrozyme^{tPA} {CH_3SO_2-D-HHT-Gly-Arg-*p*NA} and Spectrozyme^{UK} {Cbo-L-(γ)Glu(α-*t*-BuO)-Gly-Arg-*p*NA} were obtained from American Diagnostica Inc. (Greenwich, CT), and S-2222 {Bz-Ile-Glu[γ-O(H or CH_3)]-Gly-Arg-*p*NA} was from Chromogenix (Milan, Italy). Chromatography materials were from Amersham Pharmacia Biotech (Uppsala, Sweden). Bovine trypsin and porcine pancreatic elastase (type IV) were from Sigma. Oligonucleotides were synthesized and provided in HPLC-purified form by Cruachem. Reagents for peptide synthesis were purchased from Advanced ChemTech (Louisville, KY) or Burdick and Jackson Chemical Co. All other reagents were analytical reagent grade or better and obtained from Sigma.

Recombinant PAI-1 Mutagenesis, Expression, and Purification. The preparation of recombinant human PAI-1 in the pET-24d vector (Novagen) has been previously described (*12*). The S338C (P9 Cys) and W175F mutations were engineered by site-directed mutagenesis using the Muta-Gene Phagmid In Vitro Mutagenesis kit (Bio-Rad) and the method of Kunkel (*27*, *28*). Mutagenic oligos $5'_{1098}$-dGACTATGACAGCTGTACATGAGGAGGCCACCG-$3'_{1067}$ and $5'_{609}$-dGGGGAAGGGAGTCTTGAACTGGCCGTTGAAGT-$3'_{578}$ were used to make the P9-Cys and W175F variants, respectively. Mutations were confirmed by DNA sequencing of the full-length PAI-1 gene. Mutant and wild-type (wt) PAI-1 constructs were expressed in *Escherichia coli* strain BL21(DE3)pLysS and purified as described previously (*12*). P9-Cys PAI-1 and the double mutant variant, W175F/P9-Cys PAI-1, were labeled with IANBD amide as described previously (*29*) with a labeling efficiency that was typically 1−1.2 mol of NBD per mole of PAI-1 variant. To remove latent PAI-1 that accumulated during the labeling reaction, labeled PAI-1 variants were subsequently purified by affinity chromatography on immobilized β-anhydrotrypsin. β-Anhydrotrypsin was prepared as described previously (*30*), and

20 mg was coupled to a 1 mL NHS-activated HiTrap column (Pharmacia) using the conditions recommended by the manufacturer. Active PAI-1 variants were bound to the β-ahydrotrypsin column in standard HEPES/NaCl buffer (pH 7.4) and step eluted with a buffer containing 10 mM NaCi, 120 mM NaCl, and 1 mM EDTA (pH 2.5). The final P9-NBD-labeled preparations were shown to be >98% active by SDS−PAGE analysis (*12*). PAI-1 protein concentrations were measured at 280 nm, using an M_r of 43 000 and extinction coefficients of 0.93 mL mg^{-1} cm^{-1} for wt PAI-1 (*31*, *32*) or 0.83 mL mg^{-1} cm^{-1} for W175F PAI-1, a value which was calculated from the A_{280} absorbance of purified W175F PAI-1 and a protein concentration determined by the Bradford dye binding assay (Bio-Rad) using a known concentration of wt PAI-1 as the standard (*33*). Far- and near-UV CD spectra were recorded with an Aviv 60DS circular dichroism spectrometer exactly as described previously (*12*).

Preparation of Peptide-Blocked Substrate PAI-1 and Peptide Synthesis. Active wt PAI-1 or W175F PAI-1 is converted into a substrate for proteinases by insertion of the octapeptide Ac-TVASSSTA into β-sheet A (*12*, *26*). Peptide-blocked PAI-1 variants were prepared essentially as described previously (*12*) with the final product determined to be more than 95% substrate by SDS−PAGE analysis (*12*). The Ac-TVASSSTA peptide was synthesized using a multiple-peptide synthesizer (Advanced ChemTech, model 348Ω) using Fmoc/Bu^t chemistry on 150 mg (0.12 mmol) of preloaded Fmoc-Ala-Wang resin (0.8 mmol/g, 100−200 mesh). N^{α}-Fmoc deprotection was performed with 25% piperidine in DMF. Individual amino acid couplings were accomplished by mixing a 5-fold excess of the Fmoc amino acid, 0.9 equiv of HBTU, and 2 equiv of DIPEA with the resin for 45 min. The N-terminal Thr was capped using a 10-fold excess of acetic anhydride and pyridine. Cleavage from the resin and deprotection of the side chains were accomplished with 3 mL of TFA in the presence of a phenol/ethanedithiol/thioanisole/water mixture (82.5:5:2.5:5, v/v). The crude peptide was purified by reverse-phase HPLC on a Vydac C_{18} column (10 μm, 250 mm × 50 mm) using a linear gradient of 0.1% TFA in water (buffer A) to 0.1% TFA in acetonitrile (buffer B) over the course of 100 min. Analytical reverse-phase HPLC was performed on a Supelco Discovery Series C_{18} column (5 μm, 150 mm × 4.6 mm) using a 40 min gradient from 100% buffer A to 100% buffer B. Peptide purity was confirmed by electrospray mass spectrometry with a calculated mass of 764.79 g/mol and an observed mass of 765.7 g/mol ($[M + H]^+$).

Proteinases. Human recombinant tPA (Activase) and the engineered variant, TNK-tPA (Tenecteplase), were provided by Genentech Inc. (San Francisco, CA). TNK-tPA contains mutations that shift the glycosylation site at amino acid 117 to residue 103 (T103N and N117Q) and abolish the basic residue motif in the variable region-1, also known as the "37-loop", of the protease domain (K296A, H297A, R298A, and R299A) (*19*). Together, these mutations make this variant of tPA more fibrin-specific and significantly resistant to PAI-1 inactivation (~100-fold) (*19*, *20*, *34*, *35*). Both tPA preparations are largely composed of the single-chain form and were subsequently converted to the two-chain form by continuous fluxing of the tPA preparations through a 1 mL plasmin−Sepharose column as previously described (*26*). Human recombinant high-molecular weight two-chain uPA was provided by Abbott Laboratories (Chicago, IL). Bovine β-trypsin was purified from a commercial TPCK-treated preparation (Sigma catalog no. T-1426) by chromatography on SBTI−Sepharose and pH-gradient elution as previously described (*25*, *30*). Proteinase concentrations were determined from the absorbance at 280 nm using extinction coefficients of 1.93, 1.36, and 1.54 mL mg^{-1} cm^{-1} and M_r values of 63 500, 54 000, and 23 900 for tPA or TNK-tPA, uPA, and β-trypsin, respectively. The functional concentration of purified β-trypsin was further confirmed by active site titration with fluorescein mono-*p*-guanidinobenzoate as described previously (*30*). The concentration of the commercial porcine elastase preparation (Sigma catalog no. E-0258) was determined from the dry weight (74% protein) and an M_r of 25 900.

Stoichiometry of Inhibition. The stoichiometry of inhibition (SI), i.e., the number of moles of inhibitor required to inhibit 1 mol of proteinase, was determined from the change in fluorescence accompanying displacement of *p*-aminobenzamidine (PAB) from the active site of the proteinase by wt PAI-1 or W175F PAI-1 (*36*, *37*). This method directly observes the residual amount of active proteinase during the titration experiment in contrast to other methods used by our laboratory which have utilized linked chromogenic assays (*12*). Sequential aliquots of wt PAI-1 or W175F PAI-1 were added to a fixed amount of proteinase (0.5 μM) with 50−100, 100, 40, or 20 μM PAB for tPA, TNK-tPA, uPA, and β-trypsin experiments, respectively. Displacement of active site-bound PAB was monitored as a decrease in fluorescence in an SLM 8000 or Varian Cary Eclipse fluorimeter using an excitation wavelength of 335 nm and peak emission wavelengths of 345 nm (tPA), 368 nm (TNK-tPA), or 365 nm (uPA and β-trypsin). The fluorescence data were normalized by the relationship $(F_{obs} - F_o)/\Delta F_{max}$, where F_{obs} is the emission fluorescence at each titration point, F_o is the fluorescence in the absence of added PAI-1, and ΔF_{max} is the maximal change in fluorescence due to PAB displacement. The decrease in fluorescence emission was plotted versus the PAI:proteinase molar ratio, and the SI was calculated from the extrapolated *x*-intercept of the best-fit linear regression to the data. All titrations were repeated at least three times, and SI values are reported as an average ± SEM (standard error of the mean).

Apparent Second-Order Rate Constants for Inhibition of Proteinases by PAI-1. The apparent bimolecular inhibition rate constants (k_{app}) for the irreversible inhibition of proteinases by wt PAI-1 and W175F PAI-1 were determined by the competitive kinetic method (*38*) with the chromogenic substrates Spectrozyme^{tPA}, Spectrazyme^{UK}, and S-2222 (0.5 mM) for tPA or TNK-tPA, uPA, and β-trypsin reactions, respectively. The procedure has been described elsewhere (*12*, *25*, *26*) with reactions being performed under pseudo-first-order conditions using the following concentrations of 25−750 nM for PAI-1 variants and 2−20 nM for proteinases. The current assay conditions were optimized from those used in previous studies (*12*) to obtain better data sets for regression analysis. When accounting for the current experimental SI values, we and others found control wt PAI-1 k_{app} values were within the expected ranges observed previously (*12*, *25*, *26*). Inhibition progress curves were fit to a single-exponential function with a linear component to obtain the pseudo-first-order rate constant k_{obs}. The k_{app} was obtained

by dividing k_{obs} by the functional inhibitor concentration (i.e., corrected for SI) and then by multiplying by the factor $1 + [S_0]/K_M$ to correct for the competitive effect of the chromogenic substrate. The K_M values for each proteinase−substrate pair were determined by standard Michaelis−Menten kinetics (data not shown). The values that were used were 77.9 or 80.0, 40.0, and 38.1 μM for Spectrozyme^{tPA} (tPA and TNK-tPA), Spectrazyme^{UK} (uPA), and S-2222 (β-trypsin), respectively. Data are reported as averages of at least five independent experiments ± SEM.

Conversion to the Latent Conformation. Wild-type PAI-1 and W175F PAI-1 (4 μM) were incubated at 25 or 37 °C in parallel for various time points, and aliquots were removed and mixed with tPA (8 μM) to yield final reaction concentrations of 2 and 4 μM, respectively. Reactions were quenched and analyzed by 10% SDS−PAGE, as described previously (*12*). Data are reported as averages of at least three independent experiments ± SEM.

Association Rate Constants for the Formation of the Michaelis Complex. The association rate constant (k_{assoc}) describing the second-order formation of the initial noncovalent Michaelis complexes between PAI-1 variants and proteinases was determined under pseudo-first-order conditions by following the decrease in fluorescence accompanying displacement of PAB from the proteinase active site using stopped-flow fluorimetry (*25*, *39*). The excitation wavelength was 325 nm, and the fluorescence emission was monitored using a filter (Oriel 51260) with a cutoff below 335 nm. Final proteinase concentrations of 0.3 μM tPA, 0.3 μM TNK-tPA, 0.1 μM uPA, and 0.2 μM β-trypsin were reacted with increasing PAI-1 concentrations in the presence of constant PAB (200 μM for tPA and TNK-tPA, 40 μM for uPA, and 10 μM for β-trypsin reactions). The observed pseudo-first-order rate constants were plotted versus the effective PAI-1 concentration, obtained by dividing by the correction factor $1 + [PAB]/K_{D-PAB}$, where K_{D-PAB} was determined by titration of proteinases with PAB and fitting the resulting binding isotherms to the quadratic equation for equilibrium binding as described previously (*30*). A previously established value of 8.5 μM was used for β-trypsin reactions (*25*, *30*) and the following K_{D-PAB} values: 154.6 ± 3.4, 135 ± 5.3, and 15.0 ± 0.7 μM for tPA, TNK-tPA, and uPA, respectively (data not shown). The slope of the resulting linear dependence for k_{obs} values gives the second-order association rate constant k_{assoc}.

Stopped-Flow Analysis of the Kinetics of P9-NBD-Labeled PAI-1. Stopped-flow reactions of P9-NBD-labeled PAI-1 variants were assessed on an Applied Photophysics SX.18MV stopped-flow reaction analyzer with a thermostated syringe chamber. Excitation was at 480 nm, and a filter (Oriel 51300) with a cutoff below 515 nm was used to monitor fluorescence emission. Stopped-flow experiments were carried out as previously described under pseudo-first-order conditions with proteinases in excess over P9-NBD PAI-1 or W175F/P9-NBD PAI-1 (5−100 nM) (*12*, *29*). Reaction progress curves for elastase reactions were monophasic and best fit as a single-exponential function; however, as previously noted for tPA reactions (*29*), a biphasic increase in the fluorescence of the P9-NBD probe was observed for reactions with proteinases that were inhibited by PAI-1. Accordingly, the increase in NBD fluorescence for these reactions was best fit to a double-exponential function to obtain the pseudo-first-order rate constants (k_{obs-1} and k_{obs-2}) (*29*). The biphasic reaction was reliably characterized by both a small and large amplitude change in fluorescence, the latter corresponding to insertion of the cleaved RCL (*25*, *29*). The amplitude of the smaller fluorescence change increased with the molecular size of the trapped proteinase, representing ~25, ~10, or ~5% of the total fluorescence amplitude for tPA and TNK-tPA, uPA, and β-trypsin reactions, respectively, but yielded similar limiting k_{obs-2} values (data not shown). On the basis that the rate of major fluorescence change coincides with the rate of formation of the stable serpin−proteinase complex for tPA reactions (*25*, *29*), the smaller change in fluorescence (k_{obs-2}) was deemed to be associated with a parallel reaction such as interaction of the NBD probe with the proteinase or a slow isomerization of the fluorophore (*25*, *29*). The k_{obs} values obtained for the major increase in fluorescence (k_{obs-1}) were subsequently analyzed assuming a two-step binding mechanism (*25*) for which the dependence of k_{obs} on proteinase concentration is described by the function for a rectangular hyperbola; $k_{obs} = k_{lim}[E]_o/K_M + [E]_o$, where $[E]_o$ is the proteinase concentration, k_{lim} represents the limiting first-order rate constant for the formation of an inhibited serpin−proteinase complex, and K_M is the concentration of proteinase at which k_{obs} reaches one-half of k_{lim} and is given by $(k_{lim} + k_{off})/k_{on}$, where k_{on} and k_{off} are the forward and reverse rate constants, respectively, for formation of the noncovalent Michaelis complex (*12*, *25*, *40*).

Rapid Acid Quenching Analysis of Inhibitor and Peptide-Blocked PAI-1 Kinetics. The rates of formation of the inhibited serpin−proteinase complex between tPA (1.0 μM) and wt PAI-1 or W175F PAI-1 (4.0 μM) were determined using the rapid acid quenching technique under pseudo-first-order conditions. The rapid quenching technique and analysis of the reaction products (serpin−proteinase complex and RCL-cleaved PAI-1) is described elsewhere (*12*, *26*). Reactions of peptide-blocked substrate wt PAI-1 and W175F PAI-1 with tPA were carried out under single-turnover conditions with a saturated Michaelis complex as described previously (*26*). Substrate reactions with elastase were performed under pseudo-first-order conditions with the following concentrations of wt PAI-1 or W175F PAI-1 (1.0 μM) and elastase (5.0 μM). The limiting rate value (k_{lim}) for formation of the inhibited complex or turnover as a substrate was determined from a nonlinear least-squares fitting of reaction progress curves to the function of a first-order reaction and reported as the pseudo-first-order value ± SE (standard error) of the fit.

RESULTS

Characterization of the W175F PAI-1 Mutation by Circular Dichroism. The strong evolutionary conservation of the tryptophan residue in the breach region may indicate that the primary function of this residue is to maintain the proper serpin fold and ensure the correct folding of the serpin into a metastable conformation (*2*). Recombinant expression of functionally active W175F PAI-1 in an *E. coli* system was highly efficient and produced yields comparable to that of the wt PAI-1 protein, suggesting that this mutation did not disrupt proper folding into the metastable conformation (data not shown). To determine whether replacement of Trp175 with Phe compromised the native structure of PAI-1, we compared the far- and near-UV CD spectra of purified active

Table 1: Kinetic Parameters for wt PAI-1 and W175F PAI-1[a]

	wt PAI-1			W175F PAI-1		
proteinase	k_{app}[b] (M^{-1} s^{-1})	k_{assoc}[c] (M^{-1} s^{-1})	SI (mol of I/mol of E)	k_{app}[b] (M^{-1} s^{-1})	k_{assoc}[c] (M^{-1} s^{-1})	SI (mol of I/mol of E)
tPA	$(1.0 \pm 0.1) \times 10^7$	$(4.45 \pm 0.12) \times 10^7$	1.04 ± 0.08	$(1.5 \pm 0.2) \times 10^6$	$(4.56 \pm 0.10) \times 10^7$	1.16 ± 0.02
uPA	$(5.0 \pm 0.4) \times 10^6$	$(1.34 \pm 0.01) \times 10^7$	0.95 ± 0.01[d]	$(4.9 \pm 0.3) \times 10^6$	$(1.45 \pm 0.02) \times 10^7$	0.95 ± 0.02[d]
β-trypsin	$(2.0 \pm 0.2) \times 10^6$	$(1.95 \pm 0.04) \times 10^6$	1.19 ± 0.07	$(1.8 \pm 0.1) \times 10^6$	$(2.05 \pm 0.04) \times 10^6$	1.14 ± 0.07
TNK-tPA	$(9.2 \pm 0.4) \times 10^4$	$(8.22 \pm 0.24) \times 10^4$	1.23 ± 0.11	$(6.8 \pm 0.3) \times 10^4$	$(6.53 \pm 0.18) \times 10^4$	1.17 ± 0.13

PAI-1 variant	$t_{1/2}$ of latency at 25 °C (h)	$t_{1/2}$ of latency at 37 °C (h)
wt PAI-1	22.5 ± 0.2	2.01 ± 0.04
W175F PAI-1	394 ± 35	7.2 ± 0.3

[a] Kinetic parameters were determined in 0.03 M HEPES, 0.135 M NaCl, and 1 mM EDTA at pH 7.4 and 25 °C. All data are reported as averages of at least three independent experiments ± SEM. [b] Apparent second-order rate constants for inhibition of proteinases (k_{app}) are reported as the average of at least five independent experiments ± SEM. [c] Association rate constants (k_{assoc}) are reported ± SE of the best fit linear regression to the data assuming a zero intercept. [d] The SI values slightly less than 1.0 observed for the uPA reactions are most likely due to a small experimental error in the determination of the protease or inhibitor concentrations.

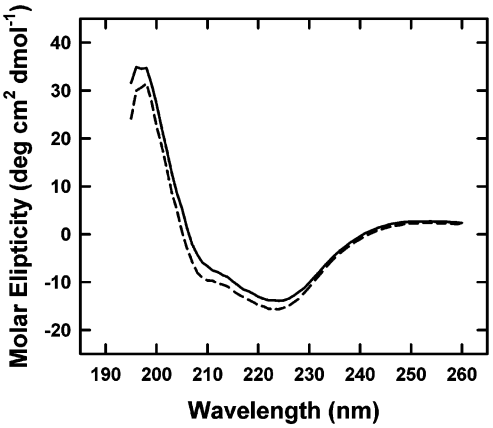

FIGURE 2: Far-UV CD spectra of wt PAI-1 and W175F PAI-1. Spectra were recorded at a concentration of 8−10 μM and 25 °C as described in Experimental Procedures: (—) wt PAI-1 and (− − −) W175F PAI-1.

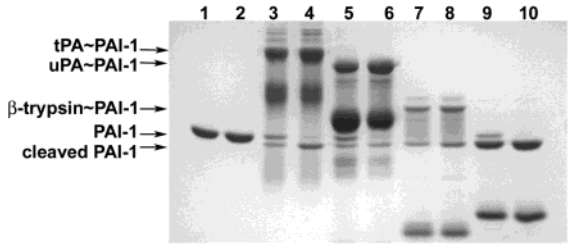

FIGURE 3: SDS−PAGE analysis of formation of the serpin−proteinase complex for wt PAI-1 and W175F PAI-1 variants. PAI-1 variants (2 μM) were reacted with a 2-fold molar excess of proteinase as described in Experimental Procedures. A total of 40 μL of each sample was resolved by 12% SDS−PAGE: lane 1, wt PAI-1; lane 2, W175F PAI-1; lane 3, wt PAI-1 and tPA; lane 4, W175F PAI-1 and tPA; lane 5, wt PAI-1 and uPA; lane 6, W175F PAI-1 and uPA; lane 7, wt PAI-1 and β-trypsin; lane 8, W175F PAI-1 and β-trypsin; lane 9, wt PAI-1 and elastase; and lane 10, W175F PAI-1 and elastase. The positions of tPA∼PAI-1, uPA∼PAI-1, and β-trypsin∼PAI-1 complexes as well as full-length and cleaved PAI-1 are indicated with arrows.

W175F PAI-1 with wt PAI-1 controls at 25 °C and pH 6.6. The profiles of the far-UV CD spectra were nearly identical, indicating that the substitution of the breach tryptophan with phenylalanine did not alter the serpin secondary structure and that the mutant W175F PAI-1 protein was properly folded (Figure 2). Near-UV CD spectra showed a decrease in molar ellipticity from 260 to 295 nm for the W175F PAI-1 variant, expected with the loss of the spectral contribution from the mutated Trp residue (data not shown).

Functional Evaluation of the W175F Mutation. To determine whether W175F PAI-1 was able to form stable serpin−proteinase complexes, reactions of wt PAI-1 or W175F PAI-1 with 2-fold molar excesses of each proteinase were analyzed by 12% SDS−PAGE. The W175F PAI-1 variant was shown to form SDS-stable complexes with tPA, uPA, and β-trypsin. With uPA and β-trypsin, this occurred without any significant increase in the relative amount of PAI-1 that is hydrolyzed as substrate, whereas with tPA, a slight increase was observed (Figure 3). Consistent with previous observations (*41*), the reaction of elastase with both wt PAI-1 and W175F PAI-1 resulted in complete hydrolysis of the respective inhibitor as a substrate. Stoichiometry of inhibition (SI) values for inhibition of all proteinases by W175F PAI-1 and wt PAI-1 were determined directly by titration of each proteinase with known concentrations of the PAI-1 variants and monitored by displacement of PAB from the active site of the proteinase as described in Experimental Procedures. The measured SI values were found to be similar to those of the wt PAI-1 controls for tPA and all other tested proteinases (Table 1). Although W175F PAI-1 was shown to be fully functional as a proteinase inhibitor (Figure 3), replacement of Trp175 with Phe appreciably altered the kinetics of the inhibitory reaction with tPA. This is clearly shown by the marked reduction of the apparent second-order rate constant (k_{app}) for inhibition of tPA, from 10.1 μM^{-1} s^{-1} with wt PAI-1 to 1.5 μM^{-1} s^{-1} with W175F PAI-1 (Table 1). The mutation had negligible effects on the k_{app} values for inhibition of uPA and β-trypsin, suggesting a proteinase-specific effect (Table 1). We have previously suggested a mechanistic involvement of the tight exosite interaction between PAI-1 and tPA in the regulation of inhibitory activity (*23*, *26*). Since there was only a slight reduction in the k_{app} value (∼35% compared to that of the wt PAI-1 control) for the reaction of W175F PAI-1 with TNK-tPA, an engineered variant lacking the major exosite interaction with PAI-1 (*20*, *24*), it is plausible that the observed proteinase-specific effects are related to differing intermolecular interactions at or near the substrate pockets of these proteinases (Table 1).

Mutation of Trp175 Retards the Spontaneous Transition to the Latent State. With the possible exception of

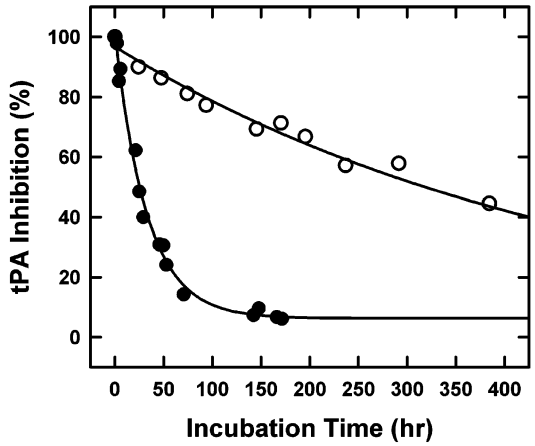

FIGURE 4: Spontaneous conversion of wt PAI-1 and W175F PAI-1 from an active to a latent conformation at 25 °C. The transition to the latent conformation was followed by monitoring the loss of inhibitory activity against tPA as a function of time for wt PAI-1 (●) and W175F PAI-1 (○). The figure shows results of representative wt PAI-1 and W175F PAI-1 experiments with $t_{1/2}$ values of 22.7 and 361 h, respectively. Averaged $t_{1/2}$ values from multiple experiments are listed in Table 1.

antithrombin (*42*) and a recently engineered α_1-antitrypsin variant (*43*), PAI-1 is the only serpin reported to spontaneously exhibit the S → R transition under physiological conditions in the absence of proteolytic cleavage (*44*, *45*). The rate of spontaneous conversion to the latent state (*44*) was monitored by the loss of inhibitory activity against tPA. Active W175F PAI-1 or wt PAI-1 was incubated at 25 or 37 °C for various lengths of time, and aliquots were removed and reacted with a 2-fold molar excess of tPA prior to SDS−PAGE analysis. The results shown in Figure 4 indicated that the Trp175 mutation significantly stabilized the active, "stressed", state of PAI-1 at 25 °C by retarding the transition to the more thermodynamically stable latent conformation, demonstrating a $t_{1/2}$ of 394 h compared to a $t_{1/2}$ of 22.5 h for wt PAI-1 controls at 25 °C (Table 1). Similarly, the latency transition was stabilized at 37 °C, but the degree of stabilization of the active conformation was reduced from 17.5-fold at 25 °C to 3.6-fold at 37 °C (Table 1). Verheyden *et al*. (*46*) have also recently reported similar latency stabilization at 37 °C with a W175F PAI-1 mutant, but did not determine the functional stability at 25 °C.

Mutation of the Breach Tryptophan Does Not Influence the Association of PAI-1 with Target Proteinases. The Trp → Phe mutation may have produced small perturbations in the orientation and flexibility of the serpin reactive center loop, as has been shown for antithrombin and heparin cofactor II in the absence of heparin (*47*, *48*). This might be expected given the proximity of the tryptophan mutation to the reactive center loop hinge (Figure 1). Association kinetics for wild-type and W175F PAI-1 reactions with tPA, uPA, and β-trypsin were determined from stopped-flow reactions by monitoring displacement of PAB from the active site of these proteinases. The linear dependencies of k_{obs} on the effective inhibitor concentrations were indistinguishable for wt PAI-1 and W175F PAI-1 reactions with these proteinases, demonstrating that the rates of formation of noncovalent Michaelis complexes (k_1 and EI in Scheme 1) were not perturbed by the tryptophan mutation near the base of the reactive center loop hinge (Figure 5 and Table 1). Except for the W175F PAI-1 reaction with tPA, the second-order

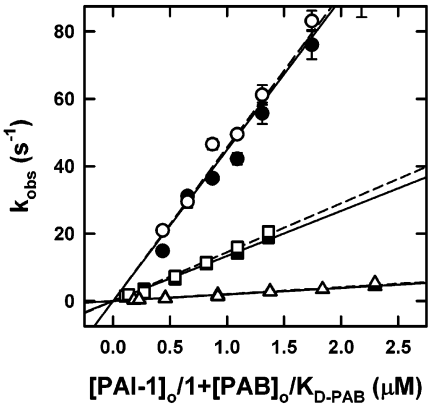

FIGURE 5: Rapid kinetics of association of wt PAI-1 and W175F PAI-1 with proteinases monitored by displacement of *p*-aminobenzamidine. Reactions of wt PAI-1 (●) and W175F PAI-1 (○) with tPA, wt PAI-1 (■) and W175F PAI-1 (□) with uPA, and wt PAI-1 (▲) and W175F PAI-1 (△) with β-trypsin were monitored in a stopped-flow experiment to obtain pseudo-first-order k_{obs} values which were plotted against the "effective" inhibitor concentration as described in Experimental Procedures. Solid (wt PAI-1) and dashed (W175F PAI-1) lines represent linear regression fits of the data assuming a zero intercept. The TNK-tPA data were excluded from the graph because the slopes and k_{assoc} values are significantly reduced compared to those of tPA, uPA, and β-trypsin. The calculated k_{assoc} values for all proteinases are presented in Table 1 and reported ±SE of the best fit linear regression line.

Scheme 1

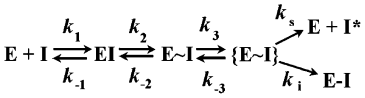

association rate constants obtained from these data were in agreement with the k_{app} values determined from competitive kinetic assays that monitor the loss of enzyme activity (Table 1). The greater than 10-fold discrepancy observed between k_{app} and k_{assoc} values for W175F PAI-1 reactions with tPA suggests the buildup of a reaction intermediate prior to loop insertion. In addition, association rates were found to be much higher in the reactions with tPA and uPA than with β-trypsin for both wt PAI-1 and W175F PAI-1 (Table 1). Previous studies have suggested that the initial binding events of PAI-1 reactions with tPA and uPA are in both cases enhanced by distal loop exosite−exosite interactions with basic surface loops on these plasminogen activators (*22*, *23*, *49*, *50*), providing an induced fit of the PAI-1 RCL into the substrate pocket of the proteinase (*51*). The data presented here showing association rates for tPA and uPA more than 10 times higher than those observed with β-trypsin, a proteinase not expected to have exosite interactions, are consistent with exosite interactions playing a significant role in the second-order association of PAI-1 with tPA and uPA, but not with β-trypsin (Table 1). Further confirmation comes from reactions with the TNK-tPA variant, in which the loss of the basic KHRR exosite motif resulted in 543- and 702-fold reductions in k_{assoc} values for wt PAI-1 and W175F PAI-1 reactions, respectively (Table 1). The slight decrease in k_{assoc} for the reaction of W175F PAI-1 with TNK-tPA compared to the control (~25%), not observed in the reaction of W175F PAI-1 with tPA, may indicate some negligible effects on the flexibility of the RCL and PAI-1 binding, but appears to be of consequence only in the absence of the exosite (*51*). Moreover, this reduction in k_{assoc} probably

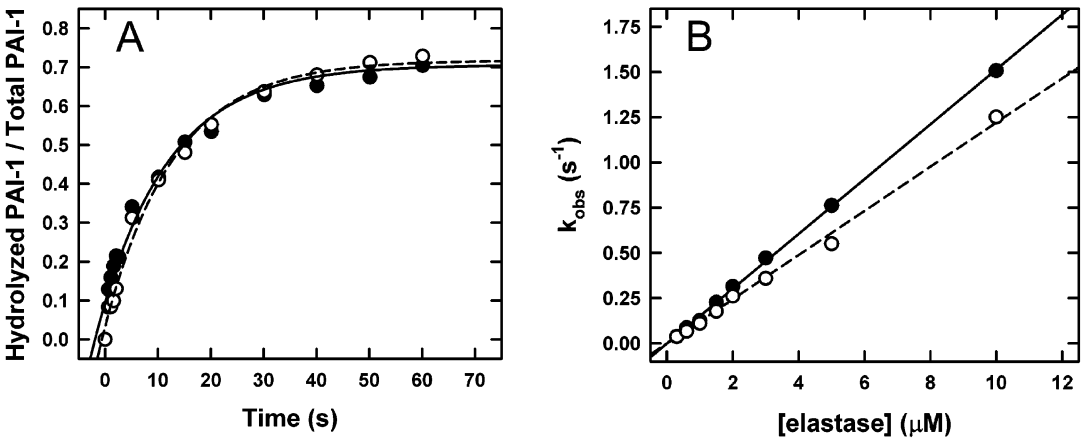

FIGURE 6: Hydrolysis of PAI-1 variants as substrates. (A) Time course for hydrolysis of Ac-TVASSSTA peptide-blocked PAI-1 variants under single-turnover conditions. Data were obtained using the rapid acid quenching technique and SDS−PAGE gel analysis. The figure shows the progressive hydrolysis of 2 μM wt PAI-1 (●) and W175F PAI-1 (○) precomplexed with the Ac-TVASSSTA peptide by 3 μM tPA at 25 °C under standard buffer conditions. The solid and dashed lines correspond to the best first-order fits to the wt PAI-1 and W175F PAI-1 data, respectively. (B) Stopped-flow analysis of the hydrolysis of P9-NBD-labeled wt PAI-1 and W175F PAI-1 as a function of elastase concentration. The data points represent averaged k_{obs} values from 6−10 wt PAI-1 (●) or W175F PAI-1 (○) experiments. Solid (wt PAI-1) and dashed (W175F PAI-1) lines represent linear regression fits of the data. The calculated values for the second-order rate of hydrolysis are described in the text.

accounts for the small effect of the W175F mutation on the k_{app} value in reactions with TNK-tPA (Table 1).

Hydrolysis of PAI-1 Variants as Substrates. To determine whether the step(s) in the tPA reaction that was altered by the W175F mutation occurred prior to or at the point of enzyme acylation, we determined the rate at which the P1−P1′ scissile bond of W175F PAI-1 was hydrolyzed by tPA. In reactions between proteinases and peptide-blocked PAI-1 variants, reactive center loop insertion is prevented due to the presence of the preinserted octapeptide in β-sheet A (*12*, *26*, *52*). By using peptide-blocked variants of wt PAI-1 and W175F PAI-1, the rate of enzyme acylation was observed directly by following the first-order increase in the amount of hydrolyzed substrate PAI-1 in a rapid quenching experiment (*26*). If acylation of the scissile peptide bond was the affected mechanistic step in the inhibitory reaction with tPA, or occurred after the affected step, the observed rate for hydrolysis of substrate W175F PAI-1 should be significantly decreased relative to that of the substrate form of wt PAI-1. To monitor directly the acylation of PAI-1 variants, the Ac-TVASSSTA-complexed substrate forms of wt PAI-1 and W175F PAI-1 (2 μM) were reacted with tPA (3 μM) under single-turnover conditions (Figure 6A). Under these conditions, the Michaelis complex was saturated by excess tPA and the acid quenching experiment followed the breakdown of the Michaelis complex into hydrolyzed inhibitor and free tPA (*26*). The tight exosite interface of the tPA∼PAI-1 Michaelis complex prompted a slow deacylation of peptide-blocked PAI-1 variants, consistent with observations in previous studies (*26*). The rate constants for acylation of substrate wt PAI-1 and W175F PAI-1 were indistinguishable, suggesting that the mutation in the breach region does not perturb loop acylation or events leading to loop acylation and therefore affects a postacylation intermediate step (Table 2).

The shorter length of the cleaved RCL following hydrolysis at the P3−P4 bond by elastase prevents proteinase trapping in a stable acyl−enzyme complex, and thus, the PAI-1 variant becomes turned over as a substrate (see Figure 4) (*41*, *53*). This feature permitted the observation of scissile bond catalysis and loop insertion in the absence of proteinase trapping without the need to block loop insertion with an exogenous peptide that induces an expansion of β-sheet A (*12*). The turnover of both P9-NBD PAI-1 and W175F/P9-NBD PAI-1 as substrates was linear with proteinase concentration over the tested range (Figure 6B). Second-order rate constants calculated from the slopes of the linear dependencies were 1.5×10^5 and 1.2×10^5 M^{-1} s^{-1} for P9-NBD PAI-1 and W175F/P9-NBD PAI-1, respectively, indicating that both PAI-1 variants were cleaved as substrates by elastase at essentially similar rates. The corresponding unlabeled proteins were hydrolyzed as substrates by elastase at nearly the same rates (Table 2), in excellent agreement with the P9-NBD studies.

Table 2: Substrate Hydrolysis of wt PAI-1 and W175F PAI-1[a]

	k_{obs} (s^{-1})	
proteinase	wt PAI-1	W175F PAI-1
tPA[b]	0.08 ± 0.01	0.08 ± 0.01
elastase[c]	0.73 ± 0.12	0.91 ± 0.06

[a] Measured from the rapid quenching experiments in 0.03 M HEPES, 0.135 M NaCl, and 1 mM EDTA at pH 7.4 and 25 °C. [b] Measured using Ac-TVASSSTA peptide-blocked PAI-1 variants. Data are reported as ±SE of the best first-order fit to the rapid quench data. [c] Measured using wt PAI-1 and W175F PAI-1 in the absence of β-sheet A blocking peptides.

The Limiting Rate of the Serpin−Proteinase Reaction Is Sensitive to the Breach Tryptophan Mutation. We utilized a well-described model (*29*) for investigating the limiting rate (k_{lim}) of serpin−proteinase reactions in which the PAI-1 molecule was labeled on the P9 residue with the fluorophore NBD to follow the rate of reactive center loop insertion by stopped-flow fluorimetry. Previous studies have documented that the inhibitory activity of P9-NBD PAI-1 is mostly unchanged by the presence of the fluorophore and similar to that of unlabeled wt PAI-1 (*25*, *26*, *29*, *39*). Reactions of both wt P9-NBD PAI-1 and W175F/P9-NBD PAI-1 with tPA, uPA, or β-trypsin were biphasic. The observed rate of reaction for the greatest amplitude change corresponded to reactive center loop insertion (k_{obs}) (*29*), whereas the minor

Table 3: Individual Rate Constants for Proteinase Inhibition by wt PAI-1 and W175F PAI-1[a]

	wt PAI-1				W175F PAI-1			
proteinase	k_{lim} (s^{-1})	K_M (μM)	k_{lim}/K_M[b] (M^{-1} s^{-1})	$\Delta G^{\ddagger}$[c] (kcal/mol)	k_{lim} (s^{-1})	K_M (μM)	k_{lim}/K_M (M^{-1} s^{-1})	$\Delta G^{\ddagger}$[c] (kcal/mol)
tPA	3.4 ± 0.1	0.29 ± 0.03	1.2×10^7	16.7	0.10 ± 0.02	0.022 ± 0.001	4.5×10^6	18.8
uPA	22.8 ± 0.2	2.6 ± 0.1	8.8×10^6	15.6	15.1 ± 0.2	2.4 ± 0.1	6.3×10^6	15.9
β-trypsin	93.6 ± 1.9	26.1 ± 1.0	3.6×10^6	14.8	62.9 ± 0.8	19.6 ± 0.6	3.2×10^6	15.0

[a] Rapid kinetic experiments were carried out in 0.03 M HEPES, 0.135 M NaCl, and 1 mM EDTA at pH 7.4 and 25 °C. Data are reported as the best fit to the stopped-flow data ± SE of the fit. Rate constants for TNK-tPA reactions could not be obtained because of the sizable K_M for reactions with PAI-1 (see the text). [b] The second-order rate constant for inhibition of proteinases by PAI-1 was calculated from the fitted stopped-flow data as k_{lim}/K_M. [c] Gibbs free energy of activation ($\Delta G^{\ddagger}$) were calculated from the k_{lim} values obtained in the stopped-flow experiments using the following relationship from ref *55*: $k_{lim} = (k_B T/h) \exp(-\Delta G^{\ddagger}/RT)$, where k_B is the Boltzmann constant, h is Planck's constant, T is temperature, and R is the gas constant.

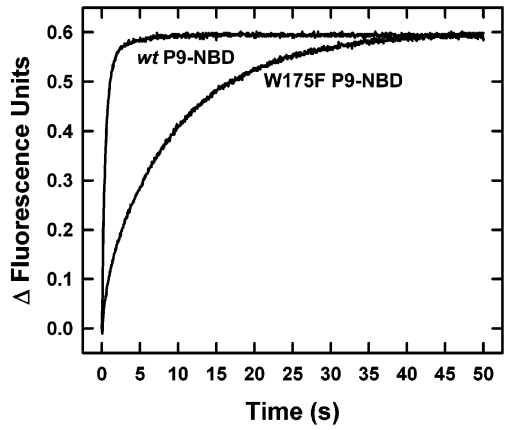

FIGURE 7: Stopped-flow analysis of inhibition of tPA by wt P9-NBD PAI-1 and W175F/P9-NBD PAI-1. Representative stopped-flow progress curves for reactions of wt P9-NBD PAI-1 or W175F/P9-NBD PAI-1 (50 nM) with tPA (2 μM) were recorded in a stopped-flow reaction analyzer as described in Experimental Procedures with 1000 data points collected over a 50 s interval. Stopped-flow reaction traces have been normalized to the same maximal fluorescence change.

amplitude change was believed to be associated with an isomerization of the fluorescent probe or a parallel interaction with the proteinase (see Experimental Procedures) (*25*, *29*). The time courses for the enhancement in fluorescence for P9-NBD PAI-1 and W175F/P9-NBD PAI-1 reactions at equivalent concentrations of tPA were consistent with mutation of the breach tryptophan significantly diminishing the observed rate of RCL insertion (Figure 7). The saturating dependencies of the pseudo-first-order rate constants for W175F/P9-NBD PAI-1 and P9-NBD PAI-1 reactions as a function of proteinase concentration for tPA, uPA, and β-trypsin are shown in Figure 8A−D and in Table 3. These findings clearly demonstrated that the limiting rate for inhibition of tPA was appreciably reduced from 3.4 to 0.10 s^{-1}, whereas the inhibition of both uPA and β-trypsin showed only modest reductions in k_{lim}, relative to those of P9-NBD PAI-1 controls (Table 3). The apparent second-order rate constants for reactions of P9-NBD-labeled PAI-1 variants with tPA, uPA, or β-trypsin, calculated as k_{lim}/K_M, were in close agreement with those determined by inhibition of proteinase activity (Table 1). If the consequence of the Trp175 → Phe mutation were simply a reduction of the intrinsic velocity of loop insertion, the reaction rates with uPA and β-trypsin would have been restricted by a common rate-limiting conformational change of the serpin topology, thus resulting in comparable k_{lim} values. On the contrary, the k_{lim} values found for inhibition of uPA and β-trypsin by W175F/P9-NBD PAI-1 were much more than 150 and 600 times greater than the observed k_{lim} for the inhibition of tPA by this mutant, strongly suggesting that the process of loop insertion remained unaffected. These observations provide compelling evidence that the inherent rate of loop insertion was not perturbed by mutation of the conserved tryptophan, but alternatively, a rate-limiting intermediate step prior to loop insertion is sensitive to the mutation for tPA and, to a minor extent, the uPA and β-trypsin reactions (Table 3).

Previous studies have recognized that formation of inhibited serpin−proteinase complexes is probably limited by the same mechanistic step that influences the rate of reactive center loop insertion and can be directly followed in a rapid quenching experiment (*12*, *26*). On the basis of the K_M values determined from the P9-NBD PAI-1 experiments described above (Table 3), reactions of 4 μM wt PAI-1 or W175F PAI-1 with 1 μM tPA saturated the enzyme. Control reactions with wt PAI-1 indicated that the formation of SDS-stable serpin−proteinase complexes was nearly complete within a time interval of 1 s, whereas with W175F PAI-1 as the inhibitor, reactions required nearly 20 s to complete (Figure 9A,B). Rapid quenching measurements gave limiting rate values almost identical to those using the same buffer conditions in the P9-NBD fluorescence experiments, fitting to 3.85 ± 0.48 and 0.23 ± 0.02 s^{-1} for wt PAI-1 and W175F PAI-1 reactions, respectively. These results demonstrated that trapping of the target proteinase in an SDS-stable complex with the inhibitor directly coincided with the event of reactive center loop insertion as monitored by the NBD fluorophore and further suggested that both events are dependent on molecular interactions affected by the mutation at Trp175.

The Limiting Rate of the Reaction of PAI-1 with tPA Is Influenced by Exosite Interactions. The TNK-tPA variant was used to determine whether the strong PAI-1∼tPA exosite ionic interaction may have contributed to the significant reduction in the rate-limiting step (k_{lim}) observed for the reaction of W175F/P9-NBD PAI-1 with tPA (Table 3). Mutation of the basic KHRR motif in the 37-loop to a tetraalanine sequence would effectively abolish most of the electrostatic interactions with the distal PAI-1 loop proposed by Madison *et al.* (*23*) except for the potential contribution of Arg304 to the exosite (*22*, *24*). Stopped-flow experiments directly comparing reactions of wt P9-NBD PAI-1 and W175F/P9-NBD PAI-1 with TNK-tPA at equivalent proteinase concentrations showed only slight decreases in the observed rates of RCL insertion (∼40−50%) over the tested concentration range (Figure 10A,B). The modest effect of the W175F mutation on TNK-tPA reactions compared to the

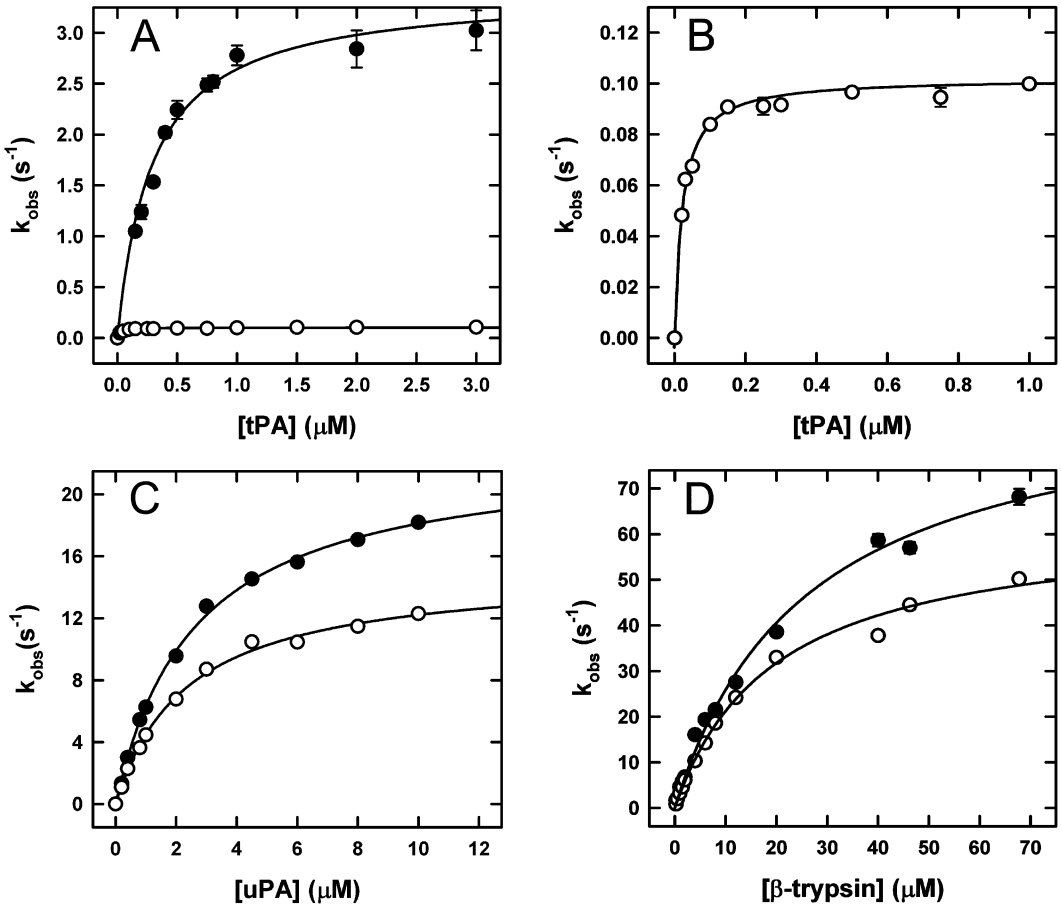

FIGURE 8: Determination of the limiting rates for proteinase inhibition. Stopped-flow analysis of reactions of wt P9-NBD PAI-1 (●) and W175F/P9-NBD PAI-1 (○) (5−100 nM) with increasing concentrations of tPA (0.05−3 μM, panels A and B), uPA (0.2−10 μM, panel C), or β-trypsin (0.25−67.7 μM, panel D) in a stopped-flow reaction analyzer as described in Experimental Procedures. Averaged k_{obs} values from 6−10 experiments were plotted and fit to the equation of a rectangular hyperbola to obtain a k_{lim} value for the reaction (Table 3). Panel B is a close-up view of the data for W175/P9-NBD PAI-1 shown in panel A.

substantial effect observed when using tPA as the target proteinase clearly establishes a central role for exosite−exosite interactions in regulating the rate-limiting step and demonstrates a close correlation between this step and molecular interactions within the breach region. Unfortunately, given the low k_{assoc} values reported in Table 1 and assuming negligible k_{off} rates, we projected that K_M values for the reactions of PAI-1 variants with TNK-tPA approach values ranging from 36.5 μM to 1.1 mM. Thus, it was not technically feasible to obtain reasonably saturated pseudo-first-order rate constants for a determination of an accurate k_{lim}. The TNK-tPA reactions could, however, be evaluated as k_{cat}/K_M using the slope of the linear increases in k_{obs} to calculate apparent second-order rate constants of 1.3×10^5 and 0.79×10^5 M^{-1} s^{-1} for wt P9-NBD PAI-1 and W175F/P9-NBD PAI-1, respectively, which were in close agreement with the k_{app} and k_{assoc} values reported in Table 1.

DISCUSSION

We have demonstrated a crucial role for the conserved breach tryptophan residue in maintaining interactions that facilitate the forward reactivity of the PAI-1 inhibition mechanism, specifically at the point in the reaction pathway where the P′-side of the distal reactive center loop must be displaced from the substrate pocket of the target proteinase for loop insertion to proceed.

The finding that a single Trp → Phe mutation within the breach region significantly decreased the rate at which tPA was inhibited by PAI-1 through considerable reductions in both k_{app} (10.1 vs 1.5 μM^{-1} s^{-1}) and k_{lim} (3.4 vs 0.1 s^{-1}) clearly supports a key role for this residue. Similar observations showing small reductions in k_{obs} or k_{lim} were observed for reactions of TNK-tPA, uPA, and β-trypsin with W175F/P9-NBD PAI-1; however, the effect was modest, consistent with the negligible effects on the overall inhibitory reaction rates (Tables 1 and 3). The lack of an effect on the formation of a noncovalent Michaelis complex (Figure 5) indicates a normal flexibility of the reactive center loop and shows that whereas the structure of the breach is important in formation of the stable acyl−enzyme complex, it does not affect the initial binding of an inhibitor to target proteinases. Our findings can best be explained when one considers the formation of tight exosite interactions between acidic residues in the distal loop of PAI-1 and basic residues found on the specificity loop of tPA (i.e., the KHRR motif in the 37-loop) (*22*, *23*, *51*). These exosite interactions were suggested to account for the reversible deacylation of the P1′ α-amino group on PAI-1 by increasing the kinetic barrier for loop insertion and therefore retarding release of the distal P′-loop of PAI-1 from the substrate pocket of tPA (*26*). The functional importance of the exosite was directly examined using the TNK-tPA variant of tPA which poorly binds PAI-1

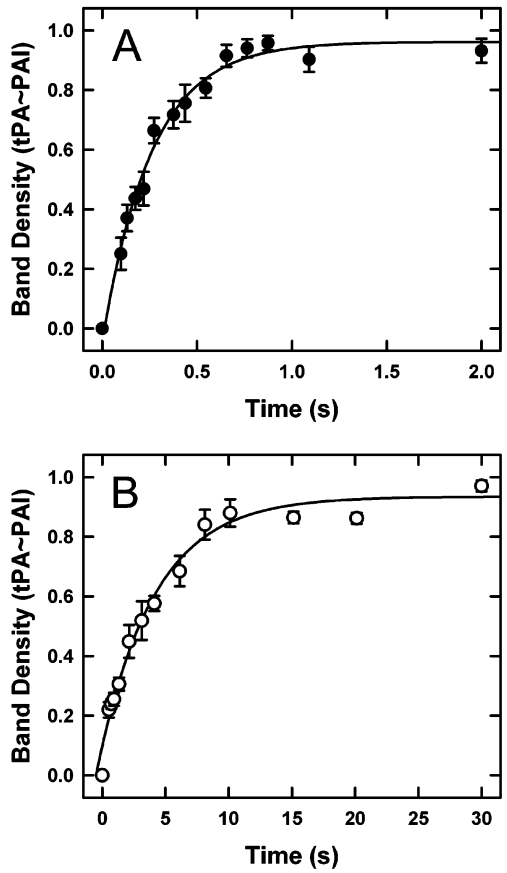

FIGURE 9: Formation of the final inhibited tPA∼PAI-1 complex. wt PAI-1 or W175F PAI-1 (4.0 μM) was reacted with tPA (1.0 μM) for various times ranging from 0.1 to 2 s (wt PAI-1, panel A) or from 0.52 to 30 s (W175F PAI-1, panel B), and the reactions were quenched with 0.12 M HCl as described in Experimental Procedures. Data points are reported as averages of at least three independent experiments ± SEM and fit to the function of a first-order reaction to obtain a k_{lim} of 3.85 ± 0.48 s^{-1} for wt PAI-1 and a k_{lim} of 0.23 ± 0.02 s^{-1} for W175F PAI-1. Band density analysis is described in Experimental Procedures.

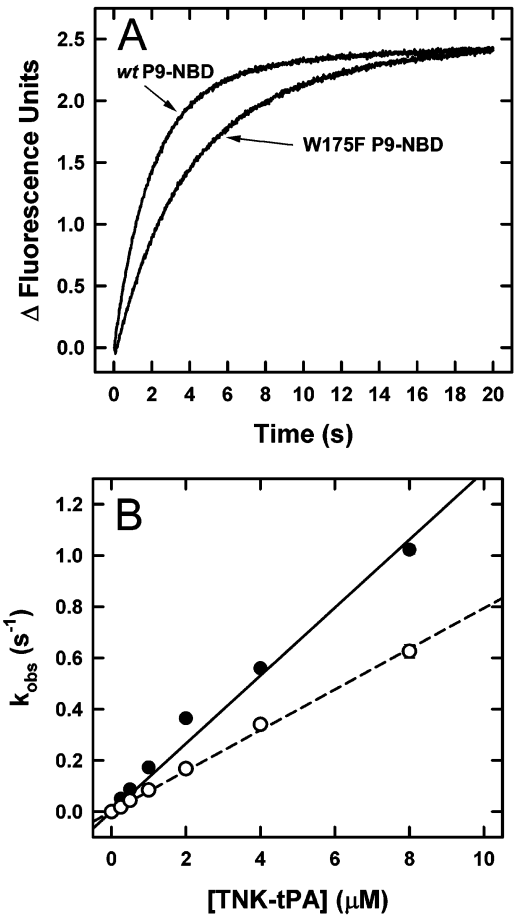

FIGURE 10: Fast reaction kinetics of inhibition of TNK-tPA by wt P9-NBD PAI-1 and W175F/P9-NBD PAI-1. (A) Representative stopped-flow progress curves for reactions of wt P9-NBD PAI-1 or W175F/P9-NBD PAI-1 (50 nM) with TNK-tPA (4 μM) were recorded in a stopped-flow reaction analyzer as described in Experimental Procedures with 1000 data points collected over a 20 s interval. Stopped-flow reaction traces have been normalized to the same maximal fluorescence change. (B) Stopped-flow analysis of reactions of wt P9-NBD PAI-1 (●) and W175F/P9-NBD PAI-1 (○) (50 nM) with increasing concentrations of TNK-tPA (0.25−8 μM) in a stopped-flow reaction analyzer as described in Experimental Procedures. k_{obs} values represent the average of 6−10 experiments. The second-order rate constant k_{cat}/K_M was calculated from linear regression fits of the data and reported in the text: (—) wt PAI-1 and (− − −) W175F PAI-1.

due to the absence of the basic KHRR motif in the exosite (Table 1 and Figure 10A,B). Like the uPA and β-trypsin experiments, the observed rates of reaction between W175F/P9-NBD PAI-1 and TNK-tPA were only moderately reduced from those of wt P9-NBD PAI-1 controls (∼40%), strongly suggesting that the large reductions in k_{app} and k_{lim} found for tPA reactions were principally a result of interactions at the exosite restricting the forward reaction rates.

When placed in the general terms of the serpin reaction mechanism (Scheme 1), our results are consistent with the postulated existence of an intermediate on the inhibitory pathway that facilitates release of the distal P′-loop (*26*). Recently, the serpin reaction model illustrated in Scheme 1 was proposed and accounts for such an intermediate step (*25*). The results presented here demonstrate the existence of this intermediate and support a model (Figure 11) in which the first critical residue(s) of the proximal loop hinge must be inserted into the breach region of β-sheet A to cause release of the distal P′-loop from the substrate cleft of the proteinase (see Figure 11 and {E∼I} in Scheme 1). According to this mechanism, formation of a noncovalent Michaelis complex (k_1/k_{-1} and EI) leads to reversible cleavage of the scissile bond (k_2/k_{-2}) and generation of the acyl−enzyme intermediate (E∼I), which triggers the initial events of loop insertion by relieving the major kinetic barrier imposed on the serpin, that of an intact reactive center loop. The structural basis of the serpin mechanism is to effectively shield the acyl−enzyme bond from aqueous deacylation, which is accomplished by retention of the newly generated P′ α-amino group at the proteinase active site. The transient intermediate step (k_3/k_{-3}) follows enzyme acylation with the first hinge residue(s) (starting with P14) being inserted into β-sheet A, an event which protects the acyl−enzyme bond from aqueous deacylation until subsequent full loop insertion rapidly traps the proteinase in an inhibited serpin−proteinase complex (k_i) and, according to the branched mechanism (*40*), releases a small amount of hydrolyzed serpin and intact proteinase (k_s). The observation that SI ($k_i + k_s/k_i$) was not compromised suggests that k_i and k_s remained unaffected by the mutation, consistent with protection of the acyl−enzyme bond in the intermediate. Experiments using the substrate PAI-1 variants suggested that the intrinsic acylation and deacylation steps

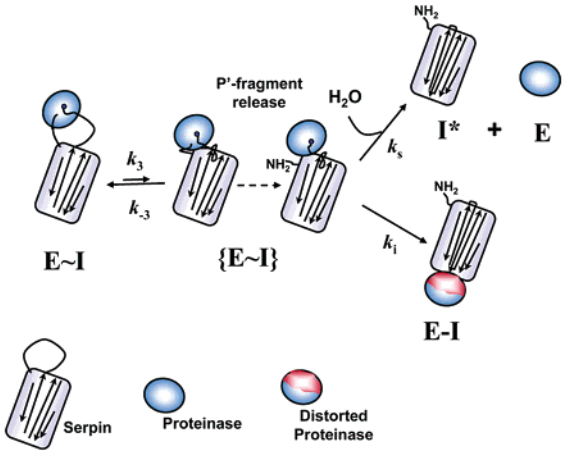

FIGURE 11: Graphical representation of the intermediate reaction step (k_3/k_{-3}) which facilitates release of the distal P′-fragment. Insertion of the first hinge residue(s) into the breach (k_3/k_{-3}) gives the intermediate ({E∼I}) with a release of the distal P′-fragment from the substrate pocket of the proteinase. This step permits complete loop insertion ($k_i + k_s$) as an inhibited serpin−proteinase complex (EI) or hydrolyzed serpin (I*) and free proteinase (E). (E∼I) represents the acyl−enzyme intermediate. Reaction steps are labeled according to Scheme 1.

(k_2/k_{-2}) were in all probability not influenced by the W175F mutation (Figure 6A). However, given that the conformational possibilities of the reactive center loop are partially restricted in the peptide-blocked variants, we cannot completely rule out this possibility. According to Scheme 1, k_{lim} is a compound rate described by the simplified expression $k_2k_3^*/(k_2 + k_{-2} + k_3^*)$, where k_3^* equals $k_3(k_i + k_s)/(k_{-3} + k_i + k_s)$ (*25*, *26*). The results herein indicating negligible effects on k_2/k_{-2}, k_i, or k_s justify the presence of a single intermediate step (k_3/k_{-3}) in the serpin mechanism that is affected by mutating the conserved breach tryptophan. On the basis of the findings presented here, we propose that Trp175 is conserved within the serpin gene family because it facilitates the first crucial step of loop insertion (Figure 11).

The slight changes in the rate constants observed for reactions of W175F/P9-NBD PAI-1 with TNK-tPA, uPA, and β-trypsin indicate that the magnitude of the mutational effect was much reduced with these enzymes (Table 3 and Figure 10). In the absence of exosite interactions, the moderate reductions in k_{lim} and k_{obs} values suggest that the binding energy of other interactions, possibly between the P1′−P3′ residues of the PAI-1 loop and their corresponding S′ pockets on the proteinase, may partially contribute to the kinetic barrier restricting release of the P′-loop. In the case of TNK-tPA reactions, potential contacts between the distal PAI-1 loop and the remaining positive charge at Arg304 (*24*) may also play a role in the kinetic barrier. The results with uPA were surprising since this proteinase is a known physiological target of PAI-1 (*54*) and has an exosite similar to that of tPA (*50*). Therefore, one would have expected a much greater impact on k_{lim} than we observed experimentally (Figure 8C and Table 3). Nevertheless, the specificity loop motif of uPA differs markedly from that of tPA (*50*), and the k_{assoc} values suggested a reduced binding affinity for PAI-1 (Table 2). Consequently, a weaker exosite interaction would account for a minimal kinetic barrier in the Michaelis complex impeding loop insertion. Consistent with this idea, apparent energy barriers were calculated in terms of the Gibbs free energy of activation ($\Delta G^{\ddagger}$) (*55*) and demonstrate that only the energy barrier for the tPA reaction was significantly increased by the W175F mutation (∼2 kcal/mol) (Table 3).

The striking stabilization of W175F PAI-1 against latency at 25 °C (Figure 3) argues that Trp175 is essential not only for optimal inhibitory function and cleaved loop insertion but also in overcoming the sizable energy barrier restricting spontaneous loop insertion. This finding makes a clear case for common molecular interactions within the breach that participate in the earliest stages of both events. This interpretation, however, is not consistent with that of Stoop *et al.* (*56*), who have suggested the two processes are mutually exclusive. Other investigators have also shown several mutations on β-strands s2B and 3B in the proximity of Trp175 and the breach region effectively retards or accelerates the rate of the latency transition, further highlighting the importance of this structural domain in the S → R transition (*57*, *58*). In particular, mutation of Tyr228 to a serine dramatically retarded the latency transition (*57*). Although PAI-1 spontaneously inserts the complete intact loop (*44*, *45*), it is not prone to assume a conformation in which the loop is partially inserted as has been shown for antithrombin (*47*) and heparin cofactor II (*48*). Nevertheless, such an intermediate conformation in PAI-1 was hypothesized on the basis of the pronounced acceleration of the latency transition by the binding of a monoclonal antibody (MA-33B8) to an epitope that depended on an unfavorable equilibrium with an intermediate species having partial insertion of the proximal RCL (*59*). Recent identification of the major residues in this epitope now provides further evidence that antibody binding could depend on partial insertion of the loop (*60*). Stabilization of the latency transition in the W175F PAI-1 mutant can be reasonably explained by a mechanism whereby substitution of the bulky tryptophan residue with that of a smaller phenylalanine makes partial insertion of the proximal loop an even less likely event, perhaps by disrupting aromatic−aromatic stacking with the conserved Tyr228, believed to be involved in the stability of the PAI-1 molecule (*57*). This interpretation is consistent with the critically affected step in the inhibitory reaction being preinsertion of the first hinge residue(s) into the breach region (Figure 11).

Several crystallographic studies recently addressed this idea, showing that introduction of the P14 Thr/Ser residue into the breach appears to be a key molecular event leading to expansion of β-sheet A and full commitment to the S → R transition (*61*, *62*). Harrop *et al.* (*18*) proposed that the bulky aromatic rings of conserved Trp and Tyr residues in the breach region of PAI-2 maintain the optimal geometry of intramolecular hydrogen bonding networks that constrain the tops of β-stands s3A and s5A in an open conformation in preparing to accept the P14 residue of the inserting reactive center loop. Hydrogen bond networks have been discussed by Li *et al.* (*17*) with respect to the structure of serpin 1K and appear to be conserved in several other serpins. In particular, ϵN-1 of Trp175 is situated in a position to form a hydrogen bond with the carbonyl oxygen of the conserved Asn329 residue at the top of β-strand s5A (2.44 Å in PAI-1 PDB entry 1DVM) (Figure 12) (*63*, *64*). This hydrogen bond would clearly be precluded in the Trp → Phe mutant; nevertheless, a more probable outcome is that the smaller

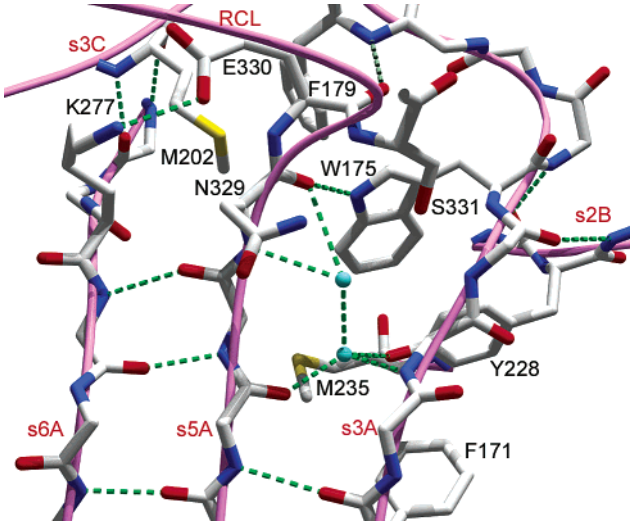

FIGURE 12: Conserved molecular interactions in the breach/hinge region of active PAI-1. Stick model (cpk coloring) showing the conserved hydrogen bonding network (green dashes) in the breach/hinge region of active PAI-1 that is maintained by the aromatic rings of Trp175 and Tyr228. The model is overlaid with a magenta α-carbon trace. Two water molecules (light blue spheres) are coordinated within the breach opening at the top of strands s3A and s5A in β-sheet A. Residue side chains are shown for selected residues in the breach region that exhibit a high degree of evolutionary conservation in the serpin gene family and are labeled using PAI-1 numbering. This figure was generated in Swiss PDB Viewer (version 3.7) (*65*), using the coordinates for active PAI-1 (PDB entry 1DVM; chain A in ref *64*).

steric size of the phenyl ring simply triggered a general disruption, or reorientation of conserved side chain packing and crucial hydrogen bonds within the core of the breach region. Alternatively, the large indole ring of tryptophan may support residue packing within the hydrophobic core of the molecule in view of a side chain orientation toward the B/C β-barrel, a domain in which mutations promoted a spontaneous latency transition in α_1-antitrypsin (*43*).

A crucial role for Trp175 and the breach region has been identified at the point in the inhibitory reaction pathway where the initial insertion of the first hinge residue(s) into β-sheet A is coupled to an intermediate reaction step ({E∼I}) that facilitates release of the distal P′-side of the loop from the active site cleft of the proteinase. The kinetic analysis of individual steps in the PAI-1 inhibition reaction using a PAI-1 mutant and multiple-target proteinases has made possible the isolation of this single step in the serpin reaction pathway which is directly linked to the structure of the serpin breach region. On the basis of past (*26*) and new results, we have proposed a model whereby the indole side chain of the breach tryptophan provides the optimal structural geometry necessary to facilitate the spring-like action of the serpin mechanism and surmount the large energy barrier that separates loop-extracted and loop-inserted serpin conformations. The biological significance of molecular interactions within the breach region is underscored by the almost ubiquitous preservation of the tryptophan residue and the well-conserved breach motif in both prokaryotic (*3*) and eukaryotic (*2*) serpins.

ACKNOWLEDGMENT

We thank Glenn Abbott, Dr. Sue Twine, and Paul Malinowski at Wilfrid Laurier University (Waterloo, ON) for expert technical assistance and data preparation for the CD studies. We also thank Drs. Steve T. Olson and Peter G. Gettins at the University of Illinois at Chicago (Chicago, IL) for critical reading and insightful comments on the manuscript.

REFERENCES

1. Silverman, G. A., Bird, P. I., Carrell, R. W., Church, F. C., Coughlin, P. B., Gettins, P. G., Irving, J. A., Lomas, D. A., Luke, C. J., Moyer, R. W., Pemberton, P. A., Remold-O'Donnell, E., Salvesen, G. S., Travis, J., and Whisstock, J. C. (2001) *J. Biol. Chem. 276*, 33293−33296.
2. Irving, J. A., Pike, R. N., Lesk, A. M., and Whisstock, J. C. (2000) *Genome Res. 10*, 1845−1864.
3. Irving, J. A., Steenbakkers, P. J., Lesk, A. M., Op Den Camp, H. J., Pike, R. N., and Whisstock, J. C. (2002) *Mol. Biol. Evol. 19*, 1881−1890.
4. Engh, R. A., Huber, R., Bode, W., and Schulze, A. J. (1995) *Trends Biotechnol. 13*, 503−510.
5. Carrell, R. W., and Stein, P. E. (1996) *Biol. Chem. Hoppe-Seyler 377*, 1−17.
6. Ye, S., and Goldsmith, E. J. (2001) *Curr. Opin. Struct. Biol. 11*, 740−745.
7. Irving, J. A., Pike, R. N., Dai, W., Bromme, D., Worrall, D. M., Silverman, G. A., Coetzer, T. H., Dennison, C., Bottomley, S. P., and Whisstock, J. C. (2002) *Biochemistry 41*, 4998−5004.
8. Al Khunaizi, M., Luke, C. J., Askew, Y. S., Pak, S. C., Askew, D. J., Cataltepe, S., Miller, D., Mills, D. R., Tsu, C., Bromme, D., Irving, J. A., Whisstock, J. C., and Silverman, G. A. (2002) *Biochemistry 41*, 3189−3199.
9. Whisstock, J. C., Skinner, R., Carrell, R. W., and Lesk, A. M. (2000) *J. Mol. Biol. 295*, 651−665.
10. Wilczynska, M., Fa, M., Karolin, J., Ohlsson, P. I., Johansson, L. B., and Ny, T. (1997) *Nat. Struct. Biol. 4*, 354−357.
11. Gettins, P. G. (2002) *Chem. Rev. 102*, 4751−4804.
12. Blouse, G. E., Perron, M. J., Thompson, J. H., Day, D. E., Link, C. A., and Shore, J. D. (2002) *Biochemistry 41*, 11997−12009.
13. Huntington, J. A., Read, R. J., and Carrell, R. W. (2000) *Nature 407*, 923−926.
14. Hopkins, P. C., Pike, R. N., and Stone, S. R. (2000) *J. Mol. Evol. 51*, 507−515.
15. Barbour, K. W., Goodwin, R. L., Guillonneau, F., Wang, Y., Baumann, H., and Berger, F. G. (2002) *Mol. Biol. Evol. 19*, 718−727.
16. Huber, R., and Carrell, R. W. (1989) *Biochemistry 28*, 8951−8966.
17. Li, J., Wang, Z., Canagarajah, B., Jiang, H., Kanost, M., and Goldsmith, E. J. (1999) *Struct. Folding Des. 7*, 103−109.
18. Harrop, S. J., Jankova, L., Coles, M., Jardine, D., Whittaker, J. S., Gould, A. R., Meister, A., King, G. C., Mabbutt, B. C., and Curmi, P. M. (1999) *Struct. Folding Des. 7*, 43−54.
19. Keyt, B. A., Paoni, N. F., Refino, C. J., Berleau, L., Nguyen, H., Chow, A., Lai, J., Pena, L., Pater, C., and Ogez, J. (1994) *Proc. Natl. Acad. Sci. U.S.A. 91*, 3670−3674.
20. Paoni, N. F., Keyt, B. A., Refino, C. J., Chow, A. M., Nguyen, H. V., Berleau, L. T., Badillo, J., Pena, L. C., Brady, K., and Wurm, F. M. (1993) *Thromb. Haemostasis 70*, 307−312.
21. Paoni, N. F., Chow, A. M., Pena, L. C., Keyt, B. A., Zoller, M. J., and Bennett, W. F. (1993) *Protein Eng. 6*, 529−534.
22. Madison, E. L., Goldsmith, E. J., Gething, M. J., Sambrook, J. F., and Gerard, R. D. (1990) *J. Biol. Chem. 265*, 21423−21426.
23. Madison, E. L., Goldsmith, E. J., Gerard, R. D., Gething, M. J., Sambrook, J. F., and Bassel-Duby, R. S. (1990) *Proc. Natl. Acad. Sci. U.S.A. 87*, 3530−3533.
24. Madison, E. L., Goldsmith, E. J., Gerard, R. D., Gething, M. J., and Sambrook, J. F. (1989) *Nature 339*, 721−724.
25. Olson, S. T., Swanson, R., Day, D., Verhamme, I., Kvassman, J., and Shore, J. D. (2001) *Biochemistry 40*, 11742−11756.
26. Kvassman, J. O., Verhamme, I., and Shore, J. D. (1998) *Biochemistry 37*, 15491−15502.
27. Kunkel, T. A., Roberts, J. D., and Zakour, R. A. (1987) *Methods Enzymol. 154*, 367−382.

28. Kunkel, T. A., Bebenek, K., and McClary, J. (1991) *Methods Enzymol. 204*, 125−139.
29. Shore, J. D., Day, D. E., Francis-Chmura, A. M., Verhamme, I., Kvassman, J., Lawrence, D. A., and Ginsburg, D. (1995) *J. Biol. Chem. 270*, 5395−5398.
30. Olson, S. T., Bock, P. E., Kvassman, J., Shore, J. D., Lawrence, D. A., Ginsburg, D., and Bjork, I. (1995) *J. Biol. Chem. 270*, 30007−30017.
31. Kvassman, J.-O., and Shore, J. D. (1995) *Fibrinolysis 9*, 215−221.
32. Vaughan, D. E., Declerck, P. J., Reilly, T. M., Park, K., Collen, D., and Fasman, G. D. (1993) *Biochim. Biophys. Acta 1202*, 221−229.
33. Bradford, M. M. (1976) *Anal. Biochem. 72*, 248−254.
34. Stewart, R. J., Fredenburgh, J. C., Leslie, B. A., Keyt, B. A., Rischke, J. A., and Weitz, J. I. (2000) *J. Biol. Chem. 275*, 10112−10120.
35. Bennett, W. F., Paoni, N. F., Keyt, B. A., Botstein, D., Jones, A. J., Presta, L., Wurm, F. M., and Zoller, M. J. (1991) *J. Biol. Chem. 266*, 5191−5201.
36. Evans, S. A., Olson, S. T., and Shore, J. D. (1982) *J. Biol. Chem. 257*, 3014−3017.
37. Olson, S. T. (1985) *J. Biol. Chem. 260*, 10153−10160.
38. Tian, W. X., and Tsou, C. L. (1982) *Biochemistry 21*, 1028−1032.
39. Komissarov, A. A., Declerck, P. J., and Shore, J. D. (2002) *J. Biol. Chem. 277*, 43858−43865.
40. Lawrence, D. A., Olson, S. T., Muhammad, S., Day, D. E., Kvassman, J. O., Ginsburg, D., and Shore, J. D. (2000) *J. Biol. Chem. 275*, 5839−5844.
41. Wu, K., Urano, T., Ihara, H., Takada, Y., Fujie, M., Shikimori, M., Hashimoto, K., and Takada, A. (1995) *Blood 86*, 1056−1061.
42. Zhou, A., Huntington, J. A., and Carrell, R. W. (1999) *Blood 94*, 3388−3396.
43. Im, H., Woo, M. S., Hwang, K. Y., and Yu, M. H. (2002) *J. Biol. Chem. 277*, 46347−46354.
44. Mottonen, J., Strand, A., Symersky, J., Sweet, R. M., Danley, D. E., Geoghegan, K. F., Gerard, R. D., and Goldsmith, E. J. (1992) *Nature 355*, 270−273.
45. Lawrence, D. A., Olson, S. T., Palaniappan, S., and Ginsburg, D. (1994) *Biochemistry 33*, 3643−3648.
46. Verheyden, S., Sillen, A., Gils, A., Declerck, P. J., and Engelborghs, Y. (2003) *Biophys. J. 85*, 501−510.
47. Huntington, J. A., Olson, S. T., Fan, B., and Gettins, P. G. (1996) *Biochemistry 35*, 8495−8503.
48. Baglin, T. P., Carrell, R. W., Church, F. C., Esmon, C. T., and Huntington, J. A. (2002) *Proc. Natl. Acad. Sci. U.S.A. 99*, 11079−11084.
49. Madison, E. L., and Sambrook, J. E. (1993) *Methods Enzymol. 223*, 249−271.
50. Adams, D. S., Griffin, L. A., Nachajko, W. R., Reddy, V. B., and Wei, C. M. (1991) *J. Biol. Chem. 266*, 8476−8482.
51. Dekker, R. J., Eichinger, A., Stoop, A. A., Bode, W., Pannekoek, H., and Horrevoets, A. J. (1999) *J. Mol. Biol. 293*, 613−627.
52. Kvassman, J. O., Lawrence, D. A., and Shore, J. D. (1995) *J. Biol. Chem. 270*, 27942−27947.
53. Zhou, A., Carrell, R. W., and Huntington, J. A. (2001) *J. Biol. Chem. 276*, 27541−27547.
54. van Meijer, M., and Pannekoek, H. (1995) *Fibrinolysis 9*, 263−276.
55. Gutfreund, H. (1995) *Kinetics for the life sciences. Receptors, Transmitters and Catalysts*, Cambridge University Press, Cambridge, U.K.
56. Stoop, A. A., Eldering, E., Dafforn, T. R., Read, R. J., and Pannekoek, H. (2001) *J. Mol. Biol. 305*, 773−783.
57. Sui, G. C., and Wiman, B. (2000) *Thromb. Haemostasis 83*, 896−901.
58. Kirkegaard, T., Jensen, S., Schousboe, S. L., Petersen, H. H., Egelund, R., Andreasen, P. A., and Rodenburg, K. W. (1999) *Eur. J. Biochem. 263*, 577−586.
59. Verhamme, I., Kvassman, J. O., Day, D., Debrock, S., Vleugels, N., Declerck, P. J., and Shore, J. D. (1999) *J. Biol. Chem. 274*, 17511−17517.
60. Gorlatova, N. V., Elokdah, H., Fan, K., Crandall, D. L., and Lawrence, D. A. (2003) *J. Biol. Chem. 278*, 16329−16335.
61. Jankova, L., Harrop, S. J., Saunders, D. N., Andrews, J. L., Bertram, K. C., Gould, A. R., Baker, M. S., and Curmi, P. M. (2001) *J. Biol. Chem. 276*, 43374−43382.
62. Saunders, D. N., Jankova, L., Harrop, S. J., Curmi, P. M., Gould, A. R., Ranson, M., and Baker, M. S. (2001) *J. Biol. Chem. 276*, 43383−43389.
63. Sharp, A. M., Stein, P. E., Pannu, N. S., Carrell, R. W., Berkenpas, M. B., Ginsburg, D., Lawrence, D. A., and Read, R. J. (1999) *Struct. Folding Des. 7*, 111−118.
64. Stout, T. J., Graham, H., Buckley, D. I., and Matthews, D. J. (2000) *Biochemistry 39*, 8460−8469.
65. Guex, N., and Peitsch, M. C. (1997) *Electrophoresis 18*, 2714−2723.

BI034737N